Fuel 182 (2016) 577–587

Contents lists available at ScienceDirect

Fuel

journal homepage: www.elsevier.com/locate/fuel

Full Length Article

Olefin upgrading under methane environment over Ag-Ga/ZSM-5 catalyst

Peng He, Yang Lou, Hua Song *

Department of Chemical and Petroleum Engineering, University of Calgary, 2500 University Dr NW, Calgary, Alberta T2N 1N4, Canada

HIGHLIGHTS

- A novel catalytic methanotreating process is developed to reduce olefin content.
- Olefin prefers to be converted to paraffin when methane is present over Ag-Ga/ZSM-5.
- Methane involvement into olefin upgrading reaction is evidenced via DRIFTS study.
- Methane presence favors metal dispersion and Ga migration to catalyst surface.

GRAPHICAL ABSTRACT

The model compound selected to represent cracked distillates from bitumen thermal cracking gets upgraded to saturated hydrocarbons under methane environment over Ag-Ga/ZSM-5 catalyst.

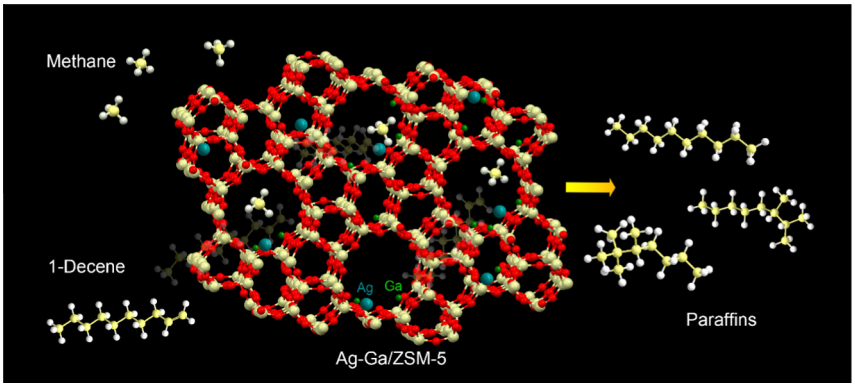

ARTICLE INFO

Article history:
Received 1 March 2016
Received in revised form 24 May 2016
Accepted 28 May 2016
Available online 10 June 2016

Keywords:
Methane
Methanotreating
Olefin
Catalytic upgrading
Cracked distillates
DRIFT

ABSTRACT

The upgrading of the petroleum cracking distillates using cheap methane rather than naturally unavailable hydrogen is an economically attractive process. This work clearly demonstrates the feasibility of methanotreating by directly using methane over zeolite-supported catalyst to convert olefins. The introduction of methane decreases the fraction of olefins and increases the fraction of paraffins in the liquid products obtained from the reaction using 1-decene as the olefin model compound when Ag-Ga/ZSM-5 is charged. It also improves the quality of liquid product in terms of higher H/C atomic ratio, higher heating value and lower bromine number. The interaction between olefins and methane on the surface of the catalyst is evidenced by DRIFT spectroscopy. When propylene is used as the olefin model compound, the shift of the peaks due to the interaction between adsorbed propylene species and catalyst surface as well as the generation of new peaks after the introduction of methane are observed. When 1-decene is used as the model compound, the suppressed intensity of —C=C— signal and enhanced alkane C—H bending peak intensity when CH_4 is present indicate the conversion of olefins into paraffins. The improved particle dispersion of the charged catalyst upon the reaction under CH_4 environment is also noticed from the TEM images, which might be closely related to its better olefin upgrading performance. The outcomes from this study might create an alternative route for cracked distillates upgrading and provide a positive attempt for more valuable methane utilization.

* Corresponding author.
E-mail address: sonh@ucalgary.ca (H. Song).

http://dx.doi.org/10.1016/j.fuel.2016.05.126
0016-2361/

1. Introduction

As the reserves of conventional petroleum cannot meet the fast increasing energy demand of human societies, non-conventional petroleum is drawing attention. Among the non-conventional petroleum sources, heavy oil could contribute a larger portion of petroleum consumption in the future due to its large reserves. For example, the remaining proven reserves of heavy oil in Canada are 165 billion barrels by the end of 2015 [1]. In 2015, the heavy oil production in Canada were 2.5 million barrels per day [1]. Heavy oil was formed from conventional oil, degraded by bacteria upon the migration towards the surface region. Some light hydrocarbons were consumed during the biological reaction process. As a result, bitumen is deficient in hydrogen and has high carbon content. Another obstacle faced by the utilization of heavy oil is its high viscosity, impeding its transportation to existing refineries, especially through pipelines [2,3]. Thermal cracking is widely employed to lower the viscosity of bitumen by breaking down the long carbon chain and complicated polycyclic molecular structure of heavy oil at high temperatures. According to the statistics released by the US Energy Information Administration, the thermal cracking capacity of the refineries in US is 3.0 million barrels per day in January, 2015 [4]. However, such treatment results in higher content of olefins which will create implementation issues such as carbon deposition during storage and transportation, incomplete combustion and generate negative environmental impacts such as photochemical smog and toxic dienes [5,6]. Olefins contained in the produced oil are oxidatively and thermally unstable and may gradually form polymeric deposit during storage [5]. Carbonaceous gum formation on the fuel injector and in the engine's intake system will lead to gasoline insufficient combustion, resulting in increased hazardous emissions such as CO, hydrocarbon, and NO_x. Moreover, these olefinic hydrocarbons may also contribute to photochemical reactions in the atmosphere, resulting in the formation of photochemical smog in susceptible urban areas. Olefins in the atmosphere can contribute to ozone formation and toxic dienes [6]. Thus, the olefins produced in the thermal cracking processes must be eliminated before the product can be sent to downstream refineries.

Hydrotreating is commonly practiced in petroleum industry to convert the olefins into saturated species, while hydrodesulfurization, hydrodenitrogenation, hydrodeoxydation and hydrodemetallization take place simultaneously in the presence of catalysts and substantial hydrogen supply [7]. According to the statistics released by US Energy Information Administration, the catalytic hydrotreating capacity in US is as large as 17.3 million barrels per day in January, 2015 [8]. However, hydrotreating process consumes expensive hydrogen, which is mainly obtained from the reforming of natural gas. The reforming of natural gas is a highly endothermic reaction and often requires high operating temperatures (>800 °C) and pressures (1.5–3.0 MPa) [9,10]. Besides the large amount of energy input, the reforming process also emits CO_2 when carbon is rejected from natural gas. If natural gas, including its recently largely discovered form (shale gas), can be directly used as the reducing agent under mild pressure, the capital and operation cost for the upgrading process would be reduced significantly. At the same time, the CO_2 emissions from steam reforming process will be avoided as carbon is incorporated into the upgraded oil rather than rejected as CO_2, thus effectively reducing the greenhouse gas contributions from petroleum industries. In 2015, the price of natural gas in US is averaged US $2.77 per million British thermal units (MBTU), while that of West Texas Intermediate (WTI) light sweet crude oil is averaged US $48.79 per barrel, which is equivalent to US $8.79 per MBTU [1]. Therefore, the incorporation of methane, the principal component of natural gas, into the synthetic oil molecules not only enhances the productivity of the product oil, but also converts the low cost methane into high value added commodities, making the process more profitable. Another disadvantage of the hydrotreating process is the high operating pressure, which is typically 70–140 atm and even higher than 200 atm [11,12], resulting in a high operating cost. If the upgrading under CH_4 atmosphere (methanotreating) could be achieved at a lowered pressure, the cost of this process would again be reduced since the pressure tolerance standard of the fabrication materials and connections of the reaction units is less strict as well as reduced energy consumption on gas compression.

In order to make the aforementioned methanotreating reactions taking place, a specially tailored catalyst system should be developed. Methane is the most inert hydrocarbon molecules due to the high C—H bond energy of 435 kJ/mol, which is the highest among all hydrocarbons, as well as the large energy gap between the highest occupied molecular orbital and lowest unoccupied molecular orbital (HOMO-LUMO) [13]. Correspondingly, the effective activation and direct conversion of methane into more commercially useful chemicals and liquid fuels represent a great challenge for the entire catalysis field. There are two main approaches for the activation and conversion of methane. The first one is to produce ethane and ethylene through the oxidative coupling of methane (OCM), which involves the presence of oxidants to make the reaction more thermodynamically favored. This approach, however, needs to improve the conversion and selectivity to meet the criteria of the industry application [13]. The other approach is to convert methane into higher hydrocarbons under non-oxidative environment. Many catalyst systems have been reported over the past three decades. Among them, zeolite supported molybdenum catalyst system demonstrates the most promising activity. Even though, less than 10% methane conversion is observed when the temperature is higher than 700 °C with major products in aromatics. The high reaction temperature and low conversion dent its commercial potential.

Choudhary et al. [14] showed that methane can be effectively converted into higher hydrocarbons and aromatics in the presence of alkenes and/or higher alkanes at low temperatures (400–600 °C) over H-galloaluminosilicate ZSM-5 type zeolite under non-oxidizing condition at atmospheric pressure. A series of related research work also demonstrates that the conversion of methane will be significantly enhanced when methane was co-fed with hydrocarbons, such as ethane, propane, pentane, hexane, light gasoline, liquefied petroleum gas, and even oxygenated hydrocarbons like methanol [15–22]. Baba et al. [23] noticed that Ag/ZSM-5 could effectively activate methane at 400 °C, and this process was assisted by the presence of C_2H_4. Gabrienko et al. [24] utilized solid-state NMR (SSNMR) to study the catalytic methane activation mechanism over Ag/ZSM-5. The SSNMR study confirmed that the cleavage of the C—H bond in methane takes place through the "carbenium" pathway, indicating that the CH_3 species was positively charged, to form methoxy groups. These results shed light on the olefin elimination using methane as the hydrogen source, because various alkanes and alkenes are generated during the olefin upgrading, which can act as promoters for methane activation. Under this condition, with specially tailored catalyst system, the methane molecules can be cleaved into H_x and CH_x, and the following engagement of these species into the unsaturated bonds would contribute to the elimination of olefins.

This paper thus studies the feasibility of olefin reduction under methane environment over Ag-Ga/ZSM-5 catalyst using 1-decene as the model compound to simulate the cracked distillates formed from heavy oil thermal cracking.

2. Experimental

2.1. Synthesis of the catalysts

NH_4-ZSM-5 with a SiO_2/Al_2O_3 ratio of 23:1 has been obtained from *Zeolyst*. The zeolite will be converted into H-ZSM-5 through calcination at 600 °C in ambient air for 5 h. The metal-modified HZSM-5 was prepared by incipient wetness impregnation method. 0.13 g $AgNO_3$ (Alfa Aesar, 99.9%) and 3.0 g $Ga(NO_3)_3{\cdot}xH_2O$ (99.9%, Alfa Aesar) were dissolved into 8 g deionized (DI) water to form the aqueous solution of the metal precursors, which was then impregnated to H-ZSM-5 for preparing 1%Ag-10%Ga/ZSM-5. The obtained wet powder was dried in the oven at 92 °C overnight, followed by calcination at 600 °C for 3 h in ambient air.

2.2. Catalytic performance evaluation

The olefin upgrading reaction was carried out in a 300 mL batch reactor manufactured by *Parr Instrument* that could tolerate high temperature up to 500 °C and high pressure up to 140 bar. In a typical run, 30 g 1-decene (Alfa Aesar, 96%) and 0.3 g Ag-Ga/ZSM-5 were put into the reactor, which was then filled with 1.0 MPa CH_4 after first purging with CH_4. The reactor was heated to and held at 350 °C, 375 °C, or 400 °C for 1 h under mechanical agitation. The control group reactions were carried out under 1.0 MPa N_2 or H_2 environment in a similar matter. After the reactor was cooled to room temperature, the liquid product was recovered by filtration to remove solid materials. The liquid yield was calculated by the weight change of the reactor with the liquid feedstock and with the liquid product.

The CHNS elementary analysis of the liquid product was carried out using an Elemental Analyzer (Perkin Elmer 2400 Series) in order to determine the weight percentage of C and H in the liquid samples. The atomic ratio of H to C was calculated from the corresponding weigh percentages.

The gas products were analyzed by an on-line four-channel micro-GC (490, Agilent) equipped with thermal conductivity detectors, which can precisely analyze H_2, O_2, N_2, CH_4, and CO in the first channel equipped with a 10 m molecular sieve 5A column; CO_2, C_2H_2, C_2H_4, and C_2H_6 in the second channel installed with a 10 m PPU column; and C_3—C_6 and $C_{3=}$—$C_{5=}$ in the third and fourth channels charged with a 10 m alumina column and a 8 m CP-Sil 5 CB column, respectively. Ar and He are the carrier gases for the first and other three channels, respectively. The carbon and hydrogen balances counting the gas and liquid products were conducted after each run with measured closures of 0.98–1.01 and 0.99–1.05, respectively.

The heating value of the liquid product was determined by an oxygen bomb calorimeter (Parr 6100 Compensated Jacket Calorimeter). The measurement was carried out at room temperature.

The Br number of liquid sample produced from each run was determined using a Metrohm 848 Titrino Plus titrator with Br number test accessories through averaging the results collected from at least three independent measurements.

2.3. Catalyst characterization

The Transmission Electron Microscopy (TEM) spectra were acquired on a Philips Tecnai TF-20 TEM instrument operated at 200 kV. An X-ray analyzer for Energy-Dispersive X-ray (EDX) spectroscopy is incorporated into the instrument for elemental analysis under STEM mode for improving image contrast between C and Ag phases. The sample was first dispersed in ethanol and supported on honey carbon on a 200 mesh Cu grid before the TEM images were recorded.

The crystalline phase compositions of prepared catalysts were examined by X-ray diffraction on a Rigaku Multiflex diffractometer with Cu Kα irradiation at a voltage of 20 kV and current of 40 mA in the 2θ of 5–50°.

The Paraffins-Olefins-Naphthenes-Aromatics (PONA) composition of the liquid samples were analyzed according to ASTM D6729 – standard test method for determination of individual component in spark ignition engine by 100 m capillary high resolution gas chromatography (GC). Representative samples of the petroleum liquid are introduced into a gas chromatograph equipped with an open tubular (capillary) column coated with the specified stationary phase. Helium carrier gas transports the vaporized sample through the column, in which it is partitioned into individual components which are sensed with a flame ionization detector (FID) as they elute from the end of the column. The detector signal is recorded digitally by way of an integrator or integrating computer. Each eluting component is identified by comparing its retention time to that established by analyzing reference standards or samples under identical conditions. The concentration of each component in mass percent is determined by normalization of the peak areas after correction of selected components with detector response factors. The unknown components are reported separately and as a summary total.

Diffuse Reflectance Infrared Fourier Transform (DRIFT) spectra were acquired by Thermo Scientific Nicolet iS50 equipped with environmental chamber and liquid-nitrogen cooled mercury–cadmium–telluride (MCT) detector. The gas inlet of a multifunctional reactor system is employed for the gas introduction to DRIFTS via Fluorinated Ethylene Propylene (FEP) tubing (Thermo Scientific, tubing 890 FEP, 8050-0125). The connection between the FEP tubing and the environmental chamber is accomplished through a short tubing with an inside diameter of 1/4 in. The gas inlet is also connected to a bubbler for liquid feedstock introduction using two three-way valves. Inlet gas could pass through the liquid sample before entering the chamber.

First, the control group DRIFT spectra were acquired at 512 scans per spectrum with a resolution of 4 cm^{-1}. The catalyst was heated to 600 °C and held for 30 min under 30 standard cubic centimeters per minute (sccm) N_2 to remove the impurities which might be adsorbed on the catalyst surface during storage. When the catalyst was cooled down to 25 °C the background spectrum was collected. Then the catalyst was heated up to 100 °C, 200 °C, 300 °C, 400 °C, 500 °C and 600 °C, respectively, and the background spectrum at each corresponding temperature was collected. When the catalyst was again cooled to 25 °C under N_2 environment after background collections, a 30 sccm propylene flow was introduced to the environmental chamber. When 1-decene instead of propylene was used as the olefin feedstock in this step, a N_2 flow was sent into a bubbler filled with liquid feedstock and kept for 10 min in order to introduce liquid feedstock into the environmental chamber as vapor phase. After that, the gas flow was switched back to 30 sccm pure N_2 through bypassing the bubbler. The catalyst was held at 25 °C for 25 min before collecting sample DRIFTS spectrum under Kubelka-Munk mode. This step was repeated at 100 °C, 200 °C, 300 °C, 400 °C, 500 °C and 600 °C, respectively. Then, the DRIFT spectra when CH_4 was present were acquired. The collection of background spectra followed the same procedure. After reactive gas introduction, the gas flow was changed to 30 sccm CH_4 for 10 min followed by 30 sccm N_2 for 15 min before collecting DRIFT spectrum. This step was again repeated at 100 °C, 200 °C, 300 °C, 400 °C, 500 °C and 600 °C, respectively, to evaluate the influence of methane presence. The spectra without the introduction of C_3H_6 or 1-decene under CH_4 environment are acquired

in a similar manner by skipping the step of introducing the olefin feedstock.

The surface acidity of the catalyst was also investigated by DRIFT spectroscopy of adsorbed pyridine during temperature programmed desorption (TPD). The catalyst sample was put in the environmental chamber under 30 sccm N_2 flow. It was pretreated at 600 °C for 30 min before collecting background spectra at 25, 100, 150, 200, 250, 300, 350, 400, 450 and 500 °C, respectively. After the chamber is cooled to 25 °C, pyridine was introduced to the sample by N_2 flow in a similar manner as the aforementioned way for 1-decene introduction. The spectra were recorded in an absorbance mode upon stabilization for 30 min at each temperature under 30 sccm N_2.

An X-ray photoelectron spectroscopy (XPS) study for the fresh and spent catalysts was carried out on a PHI Versa Probe 5000 spectrometer. The XPS spectra were taken using a monochromatic Al source (1486.6 eV) at 50 W and beam diameter of 200.0 μm with a takeoff angle of 45°. A stainless steel sample holder was used. The samples were pressed on a double sided tape, and spectra were taken with double neutralization. Survey scans were performed to identify all the elements within the sample, followed by more detailed regional scans for Ag 3d, Ga 2p, C 1s, and O 1s orbitals in order to achieve the high resolution XPS spectra for these elements of interest. A controlled-atmosphere transfer chamber was used for transferring the sample to the XPS instrument without exposure to atmosphere. The binding energies were reported relative to C 1s at ~284.8 eV.

3. Results and discussions

3.1. Catalytic performance test

1-Decene is chosen as the model compound in this study to mimic the composition of cracked distillates produced by thermal cracking of heavy oil based on a compositional analysis provided by our sponsor (data not shown due to confidential reasons). The H/C atomic ratio of the liquid products obtained at reaction temperatures of 350, 375 and 400 °C under N_2 and CH_4 environments are displayed in Fig. 1. The detailed data are also summarised in Table 1. Compared with N_2 atmosphere, the liquid product has a higher H/C atomic ratio under CH_4 environment, indicating that more H is engaged into the product molecules when CH_4 is present. When the reaction temperature is 350 °C, the H/C ratio of the liquid product under CH_4 environment is 2.02, while the H/C atomic ratio of the feedstock, 1-decene, is 2.00. The increased H/C atomic ratio indicates the saturation of —C=C— bonds and that some H is added into the product molecules.

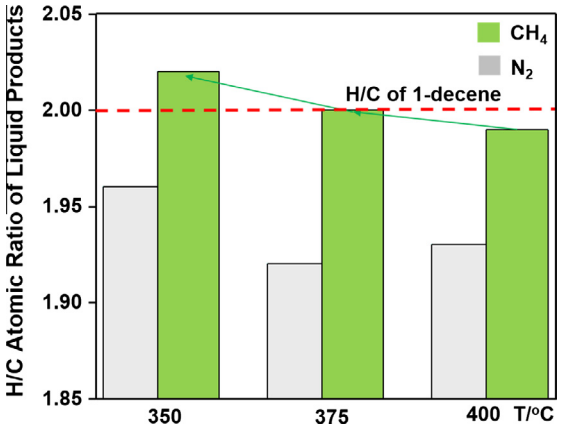

Fig. 1. H/C atomic ratio of the liquid products obtained over Ag-Ga/ZSM-5 at 350, 375 and 400 °C under N_2 and CH_4 environment.

Table 1
Liquid products obtained over Ag-Ga/ZSM-5 under variable conditions.[a]

Temperature (°C)	Gas	H/C	CH_4 conversion (%)	Bromine number (g/100 g Br)[b]	Heating value (MJ/kg)[b]	Liquid yield (%)[b]
350	CH_4	2.02	1.7	127	46.3	97.2
350	N_2	1.96	–	128	46.1	95.7
375	CH_4	2.00	1.8	111	45.9	94.1
375	N_2	1.92	–	115	45.6	92.2
400	CH_4	1.99	2.0	111	45.7	90.7
400	N_2	1.93	–	113	44.8	93.2

[a] Reaction pressure is 1.0 MPa, reaction time is 60 min.
[b] Error ranges of H/C, CH_4 conversion, bromine number, heating value and liquid yield are 0.01, 0.3, 1, 0.1 and 0.5, respectively.

It is also noticed that as the temperature is increased from 350 °C to 400 °C, the H/C atomic ratio decreases. There are possibly two competing processes proceeding simultaneously during the reaction. On one side, methane is activated by the charged catalyst to carry out the aforementioned methanotreating reaction. Upon methane cleavage, the formed H_x and C_{4-x} moieties can be engaged into the olefins and saturate the —C=C— bonds, resulting in an increased H/C atomic ratio. On the other side, the ZSM-5 based catalyst catalyzes the dehydrogenation cracking, cyclization and aromatization of the hydrocarbon molecules, resulting in a

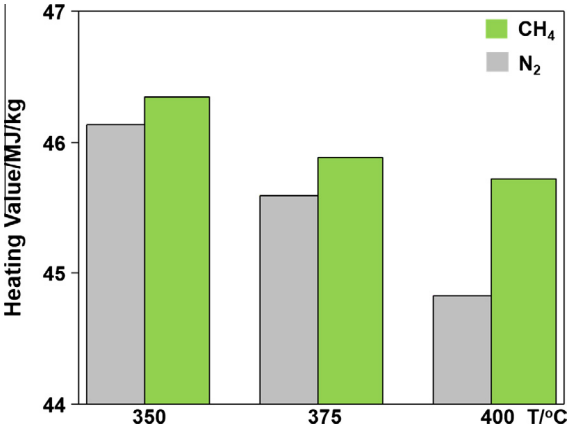

Fig. 2. Heating value of the liquid products obtained over Ag-Ga/ZSM-5 at 350, 375 and 400 °C under N_2 and CH_4 environment.

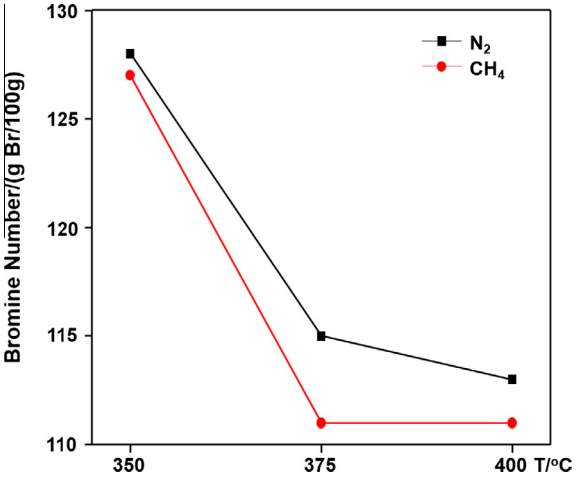

Fig. 3. Bromine number of the liquid products obtained over Ag-Ga/ZSM-5 at 350, 375 and 400 °C under N_2 and CH_4 environment.

lower H/C atomic ratio of the products. The final H/C atomic ratio of the formed liquid product is jointly determined by both processes. A higher temperature witnesses a lower H/C atomic ratio, indicating that the cracking and aromatization reactions play a more prominent role at higher temperature. A similar trend is also observed from the heating value measurement. Hydrocarbons with higher H content tends to have a higher heating value while a high C content would draw back the energy density on the basis of mass [25]. As shown in Fig. 2 (data also tabulated in Table 1), the heating values of the liquid products obtained under CH_4 atmosphere are higher than those collected under N_2 atmosphere. Again, higher heat values of the liquid products are observed at lower temperatures, where their H/C atomic ratios are also higher as evidenced in Fig. 1.

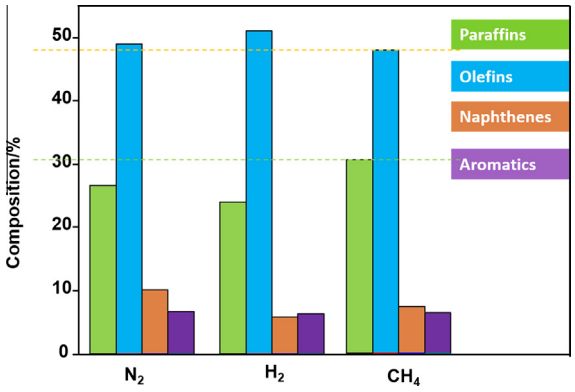

Fig. 4. The molar percentage of paraffins, olefins, naphthenes and aromatics in liquid products obtained over Ag-Ga/ZSM-5 under N_2, H_2 and CH_4 environment at 400 °C.

Table 2
The molar percentage of paraffins, olefins, naphthenes and aromatics in liquid products collected over Ag-Ga/ZSM-5 at 400 °C.

Gas	Paraffins[a]	Olefins[a]	Naphthenes[a]	Aromatics[a]
N_2	26.5	48.9	10.1	6.7
H_2	23.9	50.9	5.8	6.3
CH_4	30.5	47.8	7.4	6.4

[a] Error range: ±0.1.

The bromine number values of these liquid products are displayed in Fig. 3 and Table 1. Compared to that of its N_2 counterpart, the decreased bromine number under CH_4 environment demonstrates that more unsaturated —C=C— bonds from the 1-decene feedstock are converted when both Ag-Ga/ZSM-5 and CH_4 are present. Also, as the temperature increases, the bromine number gets notably reduced, probably due to the enhanced methanotreating reaction as well as the aforementioned aromatization process.

In order to study the catalytic olefin saturation effect due to methane presence, the liquid samples obtained at 400 °C, where the contribution of methanotreating reaction should be the most significant among all the temperatures tested, were analyzed using GC-FID for composition quantification in the sample. More than 500 species are present in each liquid sample. They are categorised into four groups, i.e. paraffins, olefins, naphthenes and aromatics. The molar percentages of the four groups in liquid products obtained using Ag-Ga/ZSM-5 under N_2, H_2 and CH_4 environment at 400 °C are demonstrated in Fig. 4 and Table 2. The presence of CH_4 with the catalyst results in the lowest olefin content along with the highest paraffin content, indicating that olefins prefers to be converted into paraffins during the catalytic methanotreating process. It is also worth noting that compared with N_2, when CH_4 is present in the reaction at 400 °C, the mole percentage of the products of C_{11}–C_{15} is increased from 5.44 to 6.17%. The fraction increase of the long carbon chain products might imply the participation of methane during the olefin upgrading reaction, and its incorporation into the carbon chains of the product oil.

3.2. Mechanistic studies

To better understand the methanotreating process, DRIFT spectra were acquired to unveil the role played by the olefin species as well as methane on the surface of the charged catalyst. First, propylene is used as the olefin model compound to probe the role played by the olefin and methane on the catalyst surface. Propylene is chosen as the model compound not only due to its simple molecular structure for easier data interpretation, but also because it contains a —C=C— double bond together with a methyl group in its structure, which could mimic the function group of olefins present in the cracked distillates. Upon the adsorption of propylene, the pattern due to C—H stretch is observed in Fig. 5a at higher wavenumber range. It is clearly noticed that when CH_4 is present,

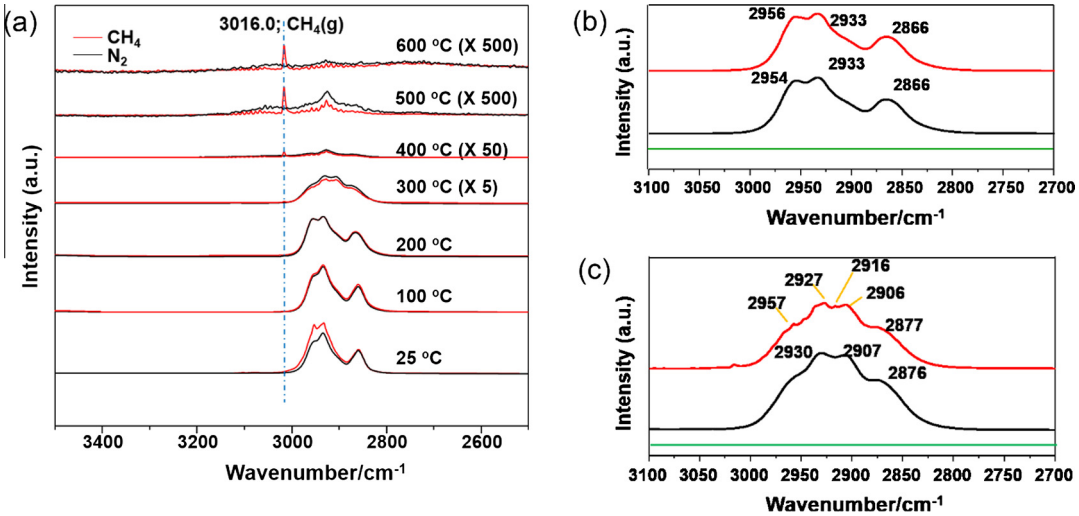

Fig. 5. DRIFT spectra acquired at higher wavenumber range upon propylene adsorption over Ag-Ga/ZSM-5 under CH_4 and N_2 atmosphere at various temperature (a), 200 °C (b) and 300 °C (c). Spectra acquired without C_3H_6 under CH_4 are displayed by the green curves. (For interpretation of the references to colour in this figure legend, the reader is referred to the web version of this article.)

the peak intensity is higher than that of its N_2 counterpart, indicating that some CH_4 is adsorbed on the surface, leading to the increased concentration of C—H bond. As the temperature gets higher, the peak intensity decays faster when CH_4 is present. A plausible explanation for this observation is that the product formed from the reaction taking place between the adsorbed propylene surface species and methane is desorbed from the catalyst surface more easily compared to the adsorbed surface reactants, which might be due to the reduced binding force between them upon the saturation of the —C=C— bonds. The interaction between CH_4 and propylene surface species is also demonstrated by the shift of the peak as well as the presence of new peaks when CH_4 is present. At 200 °C, the peak at 2954 cm^{-1} is shifted to 2956 cm^{-1} upon CH_4 introduction while the other two peaks remain the same (Fig. 5b). At this stage, the interaction between C_3H_6 and CH_4 cannot be clearly observed on the spectra. At 300 °C, the peak shift is more significant (Fig. 5c), indicating the formation of new species. A new peak at 2916 cm^{-1} is observed on the spectrum when CH_4 is present. Knozinger et al. [26] pointed out that the interactions between CH_4 and coordinatively unsaturated cations via polarization of C—H bonds can lead to symmetry reductions of methane molecules, activating its IR-forbidden vibrational modes. Among them is the symmetric stretching of methane at 2914 cm^{-1}. The new peak at 2916 cm^{-1} could origin from this vibration and exhibits a small shift from the expected position probably due to the interaction between CH_4 and the surface species including propylene surface species as well as the catalytic sites on the surface of the catalyst. Similarly, the peak due to antisymmetric stretching of CH_4 in free gas phase at 3020 cm^{-1} is also shifted to 3016 cm^{-1} (Fig. 5a) possibly as a result of the interaction between CH_4 and the surface species [26]. When only CH_4 is introduced to the catalyst, no significant peaks are observed (Fig. 5b and c, green curves), suggesting that these aforementioned peak shifts and formation are due to the synergetic effect between C_3H_6 and CH_4 upon charging the suitable catalyst.

When propylene is introduced to the catalyst, a negative peak at 1380 cm^{-1} is observed at lower wavenumber range (Fig. 6a). This peak is assigned to the suppressed bending mode of the OH···O groups in the zeolite framework as the adsorbed organic molecules bind with the —OH groups as well as the oxygen atoms exposed on the surface of the charged catalyst [27]. The peak locating at 1320 cm^{-1} might be due to the C—O bond formation during such interactions. It is also noticed that when CH_4 is present, the intensity of these peaks decays at a faster pace (Fig. 6a and b), which might be because the products formed by the reaction between CH_4 and the surface species has a weakened interaction with the catalyst. When the temperature is raised to 600 °C, the intensity of the remaining peaks, which should be due to coke formation,

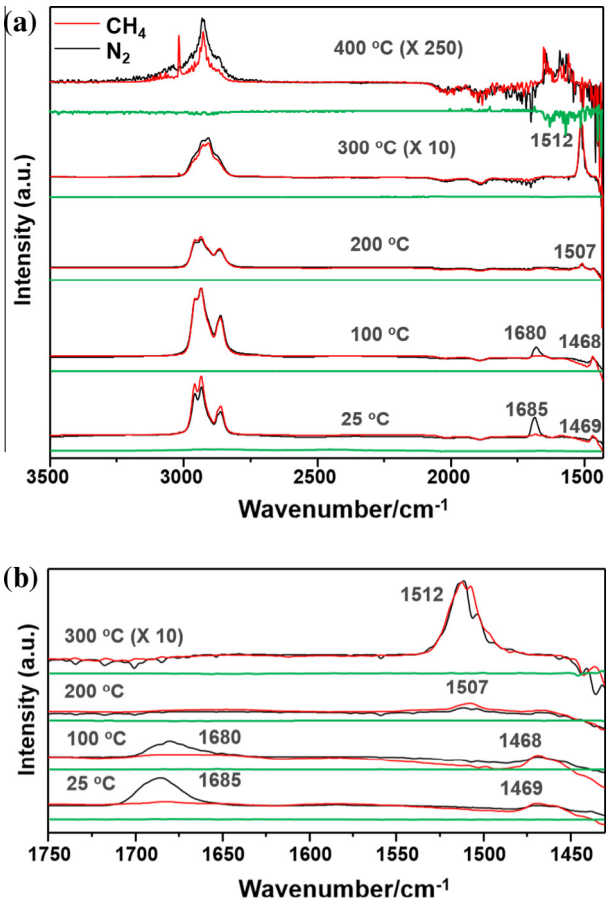

Fig. 7. DRIFT spectra acquired upon 1-decene adsorption over Ag-Ga/ZSM-5 under CH_4 and N_2 atmosphere at various temperature (a), and two regions (b, c). Spectra acquired without 1-decene under CH_4 are displayed by the green curves. (For interpretation of the references to colour in this figure legend, the reader is referred to the web version of this article.)

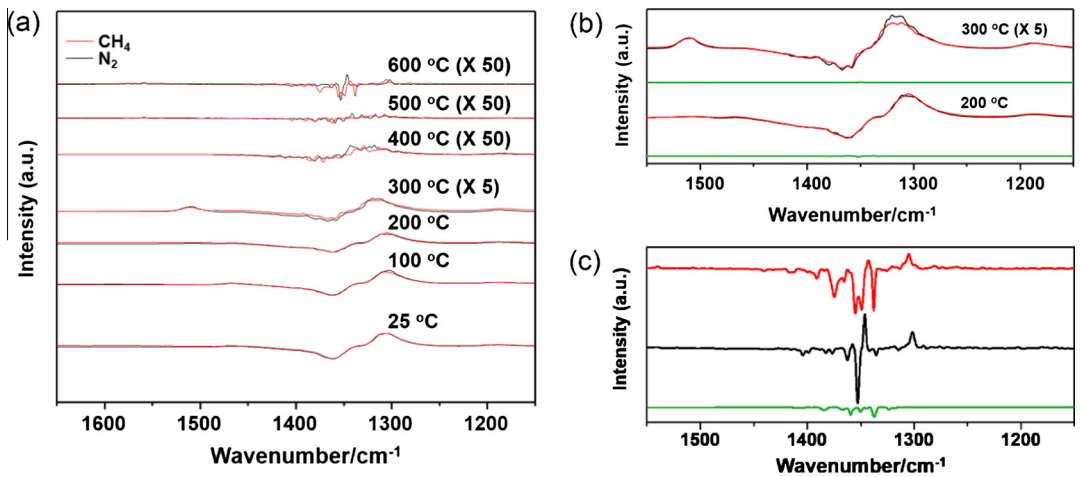

Fig. 6. DRIFT spectra acquired at lower wavenumber range upon propylene adsorption over Ag-Ga/ZSM-5 under CH_4 and N_2 atmosphere at various temperature (a), 200 °C and 300 °C (b), and 600 °C (c). Spectra acquired without C_3H_6 under CH_4 are displayed by the green curves. (For interpretation of the references to colour in this figure legend, the reader is referred to the web version of this article.)

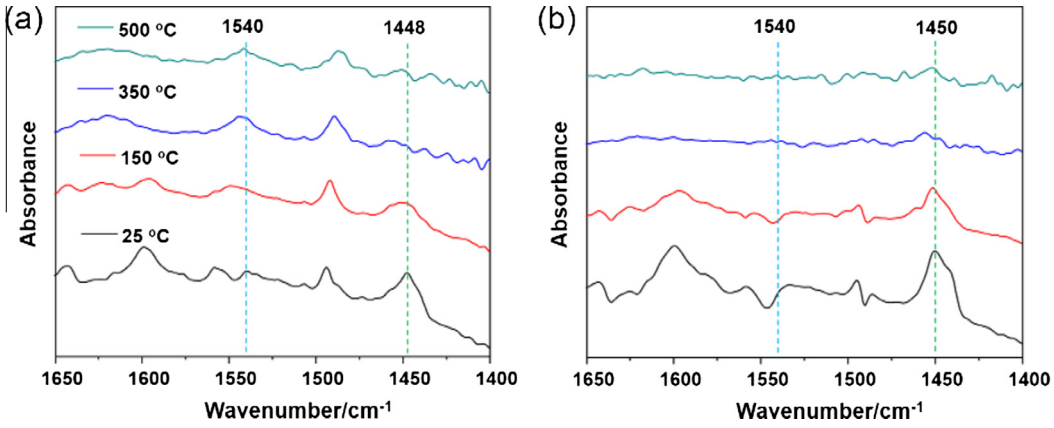

Fig. 8. The DRIFT spectra collected over the Ag-Ga/ZSM-5 during pyridine TPD.

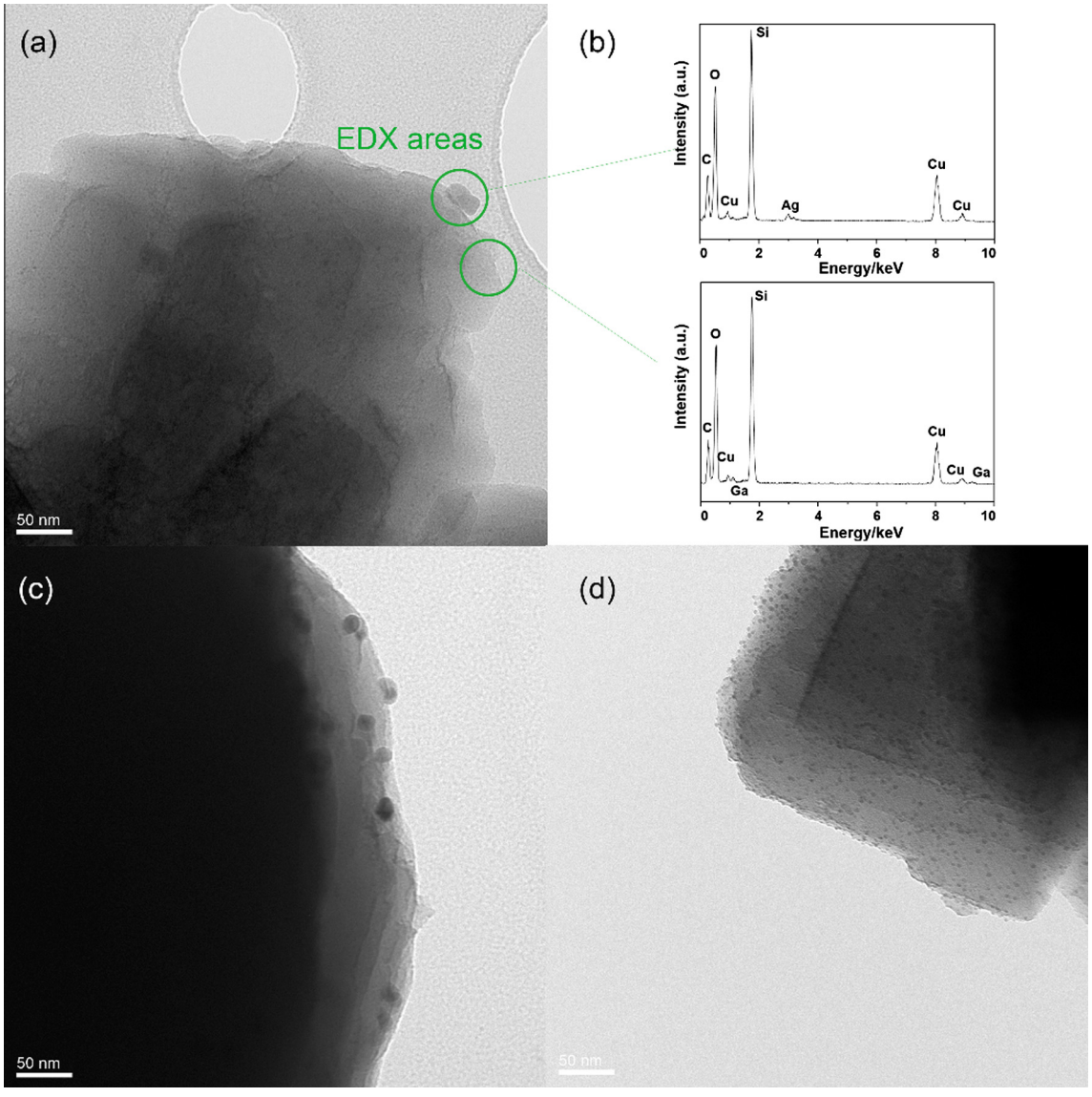

Fig. 9. TEM images of Ag-Ga/ZSM-5 (a, c, d) and the corresponding EDX spectra (b) acquired at the corresponding areas in (a).

is lower when CH_4 is present. This phenomenon implies that methane presence facilitates the coke formation minimization probably due to the enhanced H supply, thus leading to the increased catalyst lifetime and therefore benefiting the potential industrial application of the methanotreating process for olefin reduction.

Besides propylene, 1-decene, which is the feedstock for catalytic performance evaluation of this study, is also used as the olefin model compound for the DRIFT study. When the spectra collected when only CH_4 is introduced to the catalyst are referred, no recognizable peaks are observed (Fig. 7a and b, green curves). Nevertheless, when CH_4 is introduced after the introduction of 1-decene, the peak intensity due to C—H stretching is increased (Fig. 7a) in the spectrum collected at 25 °C compared with that under N_2 environment, demonstrating the possibility that some CH_4 is adsorbed on the surface with detectable amount under the assistance of co-presenting 1-decene and the concentration of C—H bond is increased as a result. It is also noticed that the pattern decays faster compared to the aforementioned DRIFT spectra recorded using propylene (Figs. 5 and 6), indicating a weaker interaction between the 1-decene and the catalyst compared to propylene. This could be because the concentration of —C=C— bonds is higher in propylene, while the interaction between —C=C— bonds with the active sites of the catalysts such as the metal cations as well as the oxygen sites is stronger than the saturated alkyl groups which are more populated in the 1-decene molecules. When methane is present, the peak intensity reduces at an even faster pace (Fig. 7a), which might be because the species produced by the reaction between CH_4 and the surface species tend to be desorbed from the surface of the catalyst.

An interesting phenomenon observed at the region between 1450 and 1750 cm^{-1} (Fig. 7b) is that under N_2 environment, the peak at 1685 cm^{-1}, which could be assigned to the stretching of —C=C—, is present. When CH_4 is present, however, this peak disappears completely even at room temperature. However, the peak at 1469 cm^{-1}, which is assigned to C—H bending mode, gets stronger. These observations exhibit the possibility that CH_4 is added to —C=C— bonds, resulting in the increased concentration of alkyl C—H bonds and thus paraffin formation under the facilitation of the Ag-Ga/ZSM-5 catalyst. The reason why such phenomenon is not observed on propylene spectra might be because the 1-decene molecule is long enough to have some double bonds away from the active sites on the catalyst surface, thus remaining quite a few double bonds untouched and IR observable, while propylene molecule is so small that the double bonds would strongly interact with the catalyst surface when the molecule is adsorbed, resulting in no double bonds left over for IR detection. This phenomenon is clearly observed at 25 and 100 °C, indicating the high activity of the charged catalyst for the activation of methane. After a closer look at the two spectra collected under CH_4 and N_2, it can be noticed that at 200 °C, these peaks disappear, and a new peak at 1507 cm^{-1} is generated when CH_4 is present, which can be assigned to C—C stretching of aromatics and grows larger as the temperature increases to 300 °C. Such observation shows that the presence of CH_4 favors the conversion of the 1-decene surface species from the perspective of aromatics formation.

3.3. Catalyst characterizations

DRIFTS is also employed in this study to evaluate the surface acidity of the developed catalyst. Fig. 8 shows the DRIFT spectra collected over HZSM-5 and the Ag-Ga loaded catalyst during pyridine TPD. The peak at around 1450 cm^{-1} is a reflection of surface Lewis acid sites [28,29]. The intensity of the peak decays gradually

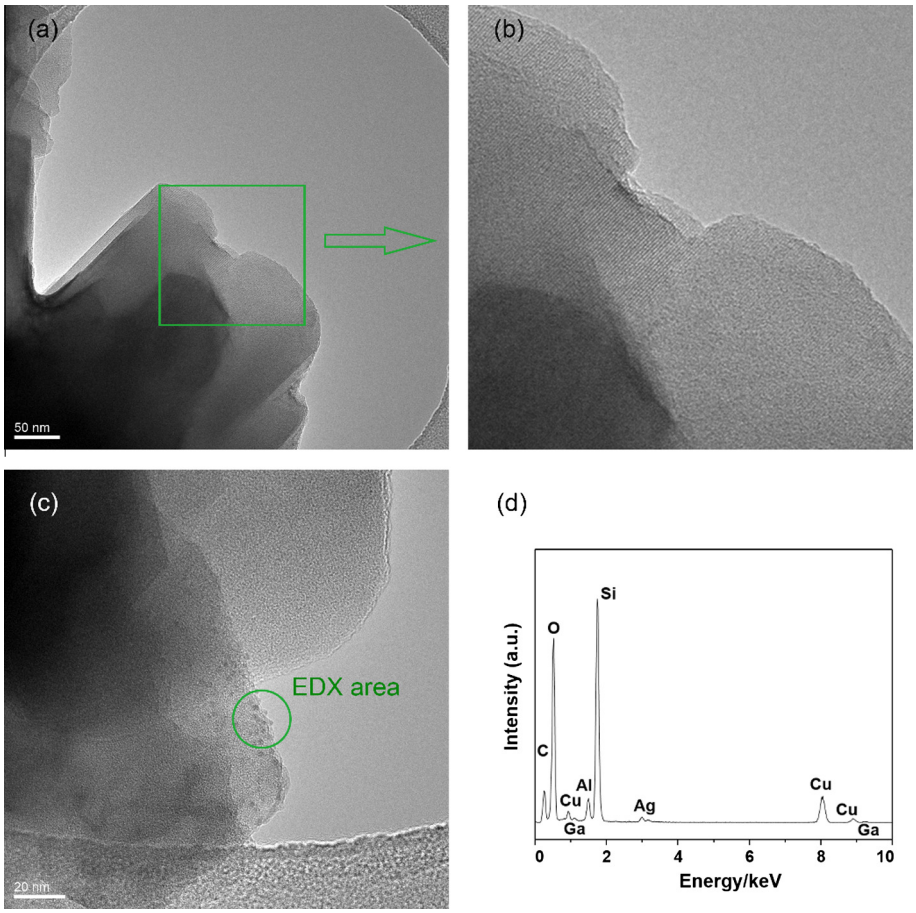

Fig. 10. TEM images of spent Ag-Ga/ZSM-5 collected after reaction with 1-decene at 350 °C under the environment of CH_4 (a–c), and the corresponding EDX spectra (d) acquired from the EDX area in (c).

as the temperature increases due to desorption of pyridine from the catalyst. The peaks in the spectrum collected at 150 °C represent the total acid sites, while the peaks remaining in the spectra recorded at 350 and 500 °C demonstrate the presence of the medium and strong forms of the acid sites, respectively. The difference indicates the amount of weak acid sites [28]. As shown in Fig. 8a, the peak due to the presence of Lewis acid sites disappears after 350 °C, indicating that the number of medium and strong Lewis acid sites in HZSM-5 is few. Therefore, the Lewis acidity present in the ZSM-5 support is dominated by weak Lewis acid sites. As displayed in Fig. 8b, however, the peak due to Lewis acid remains in the spectrum even at 500 °C, indicating that both weak and strong Lewis acid sites are still present on the surface of Ag-Ga/ZSM-5. Moreover, the peak intensity difference between the peak in the spectra acquired at 350 and 500 °C is not significant, suggesting that the number of medium Lewis acid sites might be small. Again in Fig. 8a, the peak appearing at 1540 cm^{-1} is due to the existence of Brösted acid sites upon pyridine adsorption [30]. This peak remains in the spectra up to 500 °C, implying that there are strong Brösted acid sites present in HZSM-5. However, this peak is not detectable in Fig. 8b, indicating that the concentration of Brösted acid sites is low in the Ag-Ga/ZSM-5 catalyst. These observations suggest that upon Ag-Ga loading the catalyst exhibits enhanced Lewis surface acidity and suppressed Brösted surface acidity, which might be closely related to its excellent catalytic performance towards olefin reduction under methane environment.

Fig. 9 demonstrates the morphology of the Ag and Ga particles dispersed on the fresh Ag-Ga/ZSM-5. There are some large particles with an average size of 10–20 nm (Fig. 9a and c) and lots of small particles with an average size of 3–5 nm (Fig. 9a and d). The elemental distribution on the surface of Ag-Ga/ZSM-5 is further studied by acquiring the corresponding EDX spectra of these particles (Fig. 9b). It seems that the large particles are Ag-rich while the small ones are Ga-rich after careful analysis of the collected EDX spectra.

The morphology of the spent catalyst after the reaction with 1-decene under CH_4 environment is also investigated. The crystalline of the catalyst framework stays intact and the fringe of the zeolite structure is clear (Fig. 10a and b). Fig. 10c shows the TEM image of one representative area of the spent catalyst and Fig. 10d displays the acquired EDX spectra after focusing on one specific spot with lots of small particles as shown in Fig. 10c. The averaged size of these particles is 2–3 nm, which is much smaller than that of fresh catalyst. Therefore, the dispersion of the metal species is improved after the reaction under CH_4. The EDX spectra shows that the particles are composed of both Ag and Ga. It could be concluded that the Ag-rich and Ga-rich particles in the fresh catalyst migrate towards each other and become reduced, resulting in significantly smaller alloy particles during the reaction under CH_4 environment. This phenomenon might be closely associated with the improved olefin reduction performance under CH_4 atmosphere.

Fig. 11a and c show the TEM image of two representative areas of the spent catalyst collected after the reaction under N_2 environ-

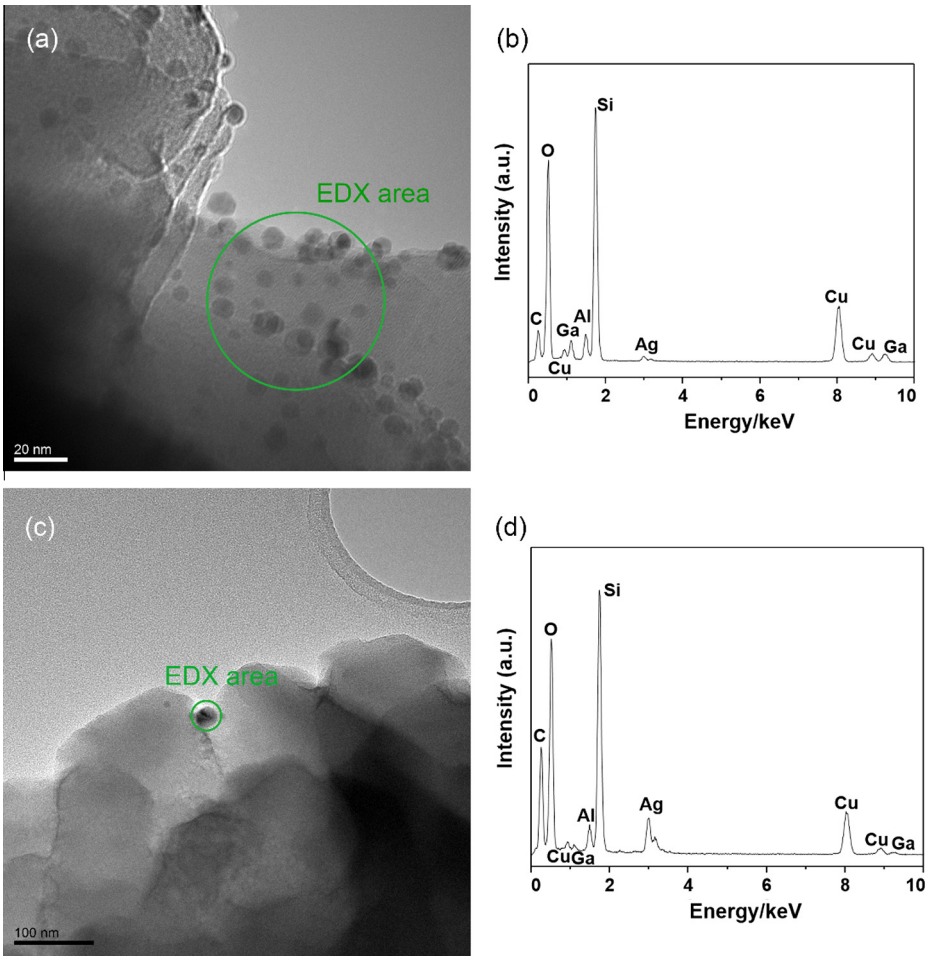

Fig. 11. TEM images of spent Ag-Ga/ZSM-5 collected after reaction with 1-decene at 350 °C under the environment of N_2 (a, c), and the EDX spectra (b, d) acquired at the corresponding EDX areas.

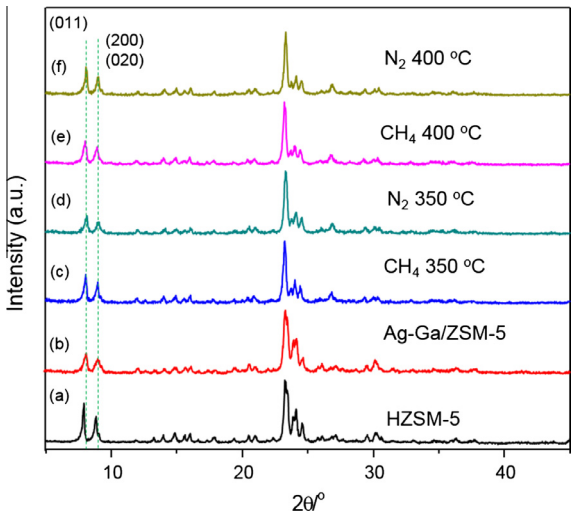

Fig. 12. XRD patterns of HZSM-5 (a), fresh Ag-Ga/ZSM-5 (b) and spent Ag-Ga/ZSM-5 under various conditions (c–f).

ment. Fig. 11b and d exhibit the EDX spectra acquired at the corresponding spots as shown in Fig. 11a and c. It is obvious to note that there are two kinds of existing particles on the surface of the spent catalyst. The small particles have an averaged size of 5–10 nm, and they are composed of both Ag and Ga. Compared with the EDX spectrum of the particles on the spent catalyst under CH_4 atmosphere (Fig. 10d), the peak intensity due to Ag is lower, while the peak intensity due to Ga is stronger. The EDX analysis results demonstrate the fact that the small particles on the spent catalyst under N_2 environment are relatively Ga-rich and might originate from the Ga-rich small particles present in the fresh catalyst (Fig. 9a and d) after particle agglomeration. Fig. 11d displays the EDX spectra after focusing on one typical large particle, which shows that the large particle is Ag-rich with averaged particle size of 20–30 nm. These large particles might also be evolved from the original large Ag-rich particles distributed in the fresh catalyst (Fig. 9a and c) after severe particle agglomeration. These TEM-EDX characterizations clearly indicate that the dispersion of the active metal species on the catalyst surface gets significantly worse after the reaction under N_2 environment, resulting in its poor catalytic performance for olefin reduction.

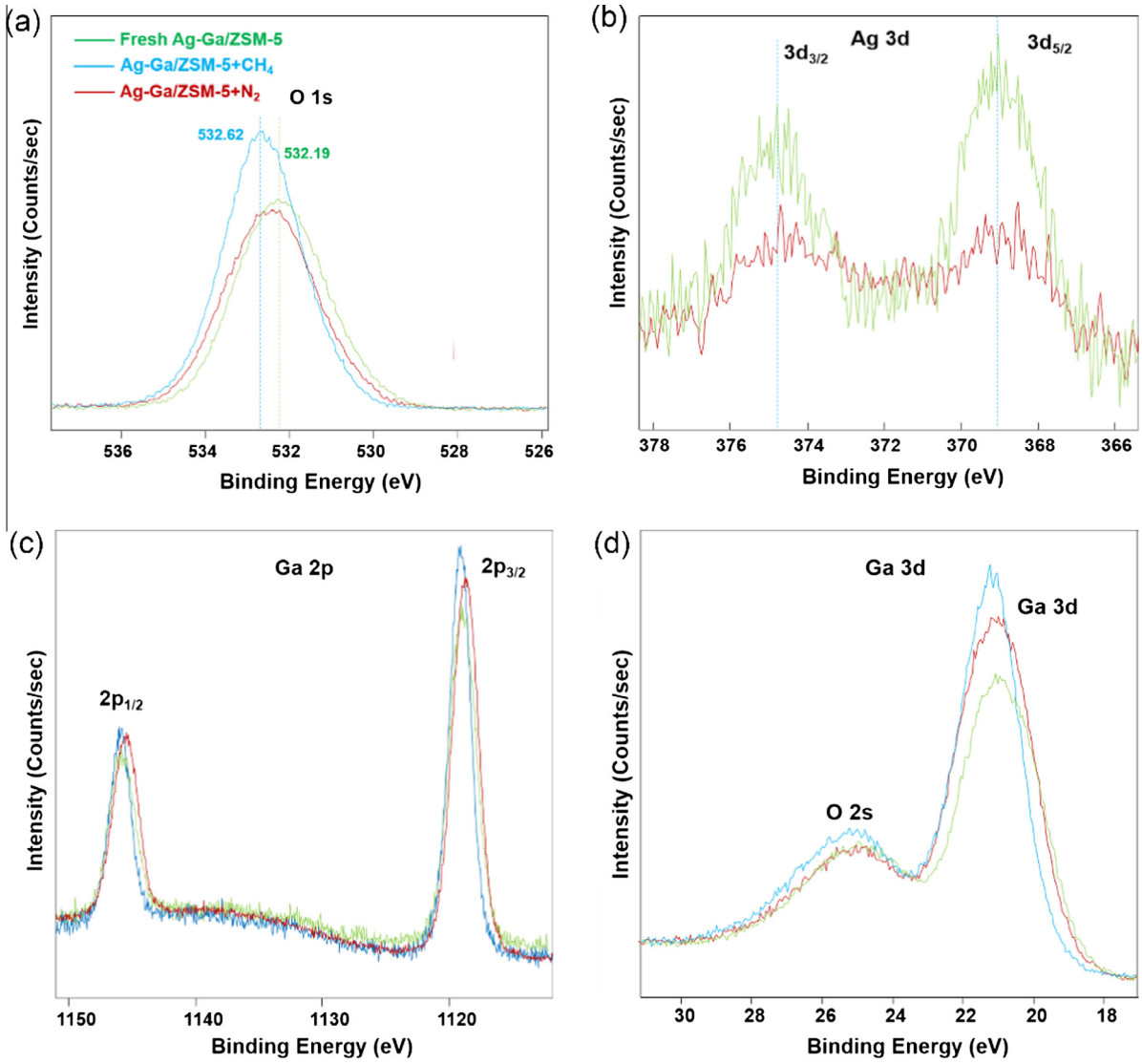

Fig. 13. XPS spectra of Ag-Ga/ZSM-5 before and after reaction with 1-decene at 1.0 MPa and 400 °C for 60 min under different environments at (a) O 1s, (b) Ag 3d, (c) Ga 2p and (d) Ga 3d regions.

The crystal phase evolution of the catalyst at various life stages is further investigated by resorting to XRD technique. Fig. 12 displays the XRD patterns of HZSM-5 support as well as fresh and spent Ag-Ga/ZSM-5 catalyst. The peaks due to the oxide compound of silver or gallium are not visible because the gallium species are well dispersed despite its high loading amount while the loading amount of silver is very low even though the particle size of the silver species is larger than gallium species. After a careful comparison, it is also worth noting that upon the introduction of Ag and Ga species into the HZSM-5 framework, the intensities of the diffraction peaks due to (2 0 0) and (0 2 0) crystal planes are significantly reduced. A plausible explanation is that the doped Ag and Ga species migrate into the HZSM-5 framework and reduce the crystalline of (2 0 0) and (0 2 0) planes.

In order to get a better understanding of how each element contained in the Ag-Ga/ZSM-5 gets distributed on the catalyst surface and their corresponding oxidation state, we have employed XPS for conducting specific scans at O 1s, Ag 3d, Ga 2p and Ga 3d regions, respectively. The results are disseminated in Fig. 13. Fig. 13a shows the XPS spectra acquired at O 1s region. After the reaction under CH_4, the surface concentration of O gets increased probably due to its diffusion from inner pores towards the surface of the zeolite support, which is evidenced by the increased peak intensities.

In a similar matter, Ga surface concentration is enhanced after upgrading reaction under CH_4 as evidenced in Fig. 13c and d, which is consistent with the hypothesis that some gallium oxide compound migrates to the surface of the catalyst. The increased binding energy of Ga, which is associated with higher valance of gallium [31,32], could be the result of such migration.

As displayed in Fig. 13b, the surface concentration of Ag gets reduced significantly after reaction probably due to its diffusion into inner pores of support, particularly under CH_4 environment, where the signal due to Ag on the surface is not visible. Based on the above observation, it can be concluded that silver species tend to diffuse into the inner pores while gallium oxide species favor the migration towards the surface of the catalyst. This phenomenon is more significant under CH_4 environment, which might be closely associated with the better catalytic performance when CH_4 is present.

4. Conclusions

The work reported here demonstrates the feasibility of upgrading of olefin with cheap methane on zeolite supported catalyst at moderate conditions to reduce the olefin content, which is crucial for commercial application. With the methanotreating applied, in addition to the increased productivity, the quality of the acquired oil product are also significantly enhanced in terms of reduced olefin content and increased paraffin content. Furthermore, the methane participation into the olefin reduction process has been evidenced experimentally by DRIFT study using propylene and 1-decene as olefin model compounds. Peak location shift, new peak formation due to methane presence, reduced olefin peak intensity as well as increased alkane peak intensity are observed when CH_4 is introduced. The good catalytic performance might be closely related to the well dispersion of metal species and migration of gallium oxide towards the surface when methane is present as well as modified surface acidity upon Ag and Ga loadings.

Acknowledgements

We gratefully acknowledge the financial supports from Meg Energy Corp. and Alberta Innovates – Energy and Environment Solutions (AI-EES, 2142).

References

[1] ST-98-2016 Alberta's energy reserves 2015 and supply/demand outlook 2016–2025. Alberta Energy Regulator; 2016.
[2] Speight JG. Heavy oil production processes. Gulf Professional Publishing; 2013.
[3] Speight JG. Petroleum refining processes. Marcel Dekker, Inc.; 2002.
[4] US Energy Information Administration webpage. <https://www.eia.gov/dnav/pet/pet_pnp_cap1_a_(na)_8CT0_BpSD_a.htm>.
[5] Bolland JL. Kinetics of olefin oxidation. Quart Rev Chem Soc 1949;3:1–21.
[6] Falls A, Seinfeld J. Continued development of a kinetic mechanism for photochemical smog. Environ Sci Technol 1978;12:1398–406.
[7] Kimura N, Iwanami Y, Sahara W, Konno S. Regenerated hydrotreatment catalyst. US patent US8795514B2; 2014.
[8] US Energy Information Administration webpage. <https://www.eia.gov/dnav/pet/pet_pnp_cap1_a_(na)_8CD0_BpSD_a.htm>.
[9] Chen Y, Mahecha-Botero A, Lim CJ, Grace JR, Zhang J, Zhao Y, et al. Hydrogen production in a sorption-enhanced fluidized-bed membrane reactor: operating parameter investigation. Ind Eng Chem Res 2014;53:6230–42.
[10] Pakhare D, Spivey J. A review of dry (CO_2) reforming of methane over noble metal catalysts. Chem Soc Rev 2014;43:7813–43.
[11] Wright MM, Daugaard DE, Satrio JA, Brown RC. Techno-economic analysis of biomass fast pyrolysis to transportation fuels. Fuel 2010;89:S11–9.
[12] Graca I, Lopes JM, Cerqueira HS, Ribeiro MF. Bio-oils upgrading for second generation biofuels. Ind Eng Chem Res 2013;52:275–87.
[13] Tang P, Zhu Q, Wu Z, Ma D. Methane activation: the past and future. Energy Environ Sci 2014;7:2580–91.
[14] Choudhary VR, Kinage AK, Choudhary TV. Low-temperature nonoxidative activation of methane over H-galloaluminosilicate (MFI) zeolite. Science 1997;275:1286–8.
[15] Choudhary VR, Mondal KC, Mulla SAR. Simultaneous conversion of methane and methanol into gasoline over bifunctional Ga-, Zn-, In-, and/or Mo-modified ZSM-5 zeolites. Angew Chem, Int Ed 2005;44:4381–5.
[16] Gabrienko AA, Arzumanov SS, Moroz IB, Toktarev AV, Wang W, Stepanov AG. Methane activation and transformation on Ag/H-ZSM-5 zeolite studied with solid-state NMR. J Phys Chem C 2013;117:7690–702.
[17] Luzgin MV, Rogov VA, Arzumanov SS, Toktarev AV, Stepanov AG, Parmon VN. Methane aromatization on Zn-modified zeolite in the presence of a Co-reactant higher alkane: how does it occur? Catal Today 2009;144:265–72.
[18] Luzgin MV, Rogov VA, Arzumanov SS, Toktarev AV, Stepanov AG, Parmon VN. Understanding methane aromatization on a Zn-modified high-silica zeolite. Angew Chem Int Ed 2008;47:4559–62.
[19] Inazu K, Koyama T, Miyaji A, Baba T. Propene production from ethene and methane using silver- and proton-exchanged zeolite catalysts. J Jpn Pet Inst 2008;51:205–16.
[20] Anunziata OA, Mercado GG, Pierella LB. Improvement of methane activation using n-hexane as Co-reactant over Zn/HZSM-11 zeolite. Catal Commun 2004;5:401–5.
[21] Anunziata OA, Mercado GVG, Pierella LB. Catalytic activation of methane using n-pentane as Co-reactant over Zn/HZSM-11 zeolite. Catal Lett 2003;87:167–71.
[22] Baba T, Inazu K. Heterolytic dissociation of C—H bond of methane over Ag^+-exchanged ceolites and conversion of methane into higher hydrocarbons in the presence of ethene or benzene. Chem Lett 2006;35:142–7.
[23] Baba T, Sawada H. Conversion of methane into higher hydrocarbons in the presence of ethylene over H-ZSM-5 loaded with silver cations. Phys Chem Chem Phys 2002;4:3919–23.
[24] Gabrienko A, Arzumanov SS, Moroz IB, Toktarev AV, Wang W, Stepanov AG. Methane activation and transformation on Ag/H-ZSM-5 zeolite studied with solid-state NMR. J Phys Chem C 2013;117:7690–702.
[25] Poddar S, Kamruzzaman M, Sujan SMA, Hossain M, Jamal MS, Gafur MA, et al. Effect of compression pressure on lignocellulosic biomass pellet to improve fuel properties: higher heating value. Fuel 2014;131:43–8.
[26] Knozinger H, Huber S. IR spectroscopy of small and weakly interacting molecular probes for acidic and basic zeolites. J Chem Soc, Faraday Trans 1998;94:2047–59.
[27] Paze C, Bordiga S, Lamberti C, Salvalaggio M, Zecchina A. Acidic properties of H-β zeolite as probed by bases with proton affinity in the 118–204 kcal mol^{-1} range: a FTIR investigation. J Phys Chem B 1997;101:4740–51.
[28] Almutairi S, Mezari B, Pidko EA, Magusin P, Hensen E. Influence of steaming on the acidity and the methanol conversion reaction of HZSM-5 zeolite. J Catal 2013;307:194–203.
[29] Yi D, Huang H, Meng X, Shi L. Adsorption-desorption behavior and mechanism of dimethyl disulfide in liquid hydrocarbon streams on modified Y zeolites. Appl Catal B Environ 2014;148–149:377–86.
[30] Xu W, Miller S, Agrawal P, Jones C. Zeolite topology effects in the alkylation of phenol with propylene. Appl Catal A Gen 2013;459:114–20.
[31] Haghofer A, Fottinger K, Girgsdies F, Teschner D, Knop-Gericke A, Schlogl R, et al. *In situ* study of the formation and stability of supported Pd_2Ga methanol steam reforming catalysts. J Catal 2012;286:13–21.
[32] Zepeda TA, Pawelec B, de Leon JND, de los Reyes JA, Olivas A. Effect of gallium loading on the hydrodesulfurization activity of unsupported Ga_2S_3/WS_2 catalysts. Appl Catal B Environ 2012;111–112:10–9.